Accelerated proximal gradient algorithm for lithium-ion battery state of charge estimation with outliers

Xixi Ji[1] · **Zili Zhang**[2] · **Yawen Mao**[1] · **Jing Chen**[1]

Abstract

In this paper, an accelerated proximal gradient based forgetting factor recursive least squares (APG-FFRLS) algorithm is proposed for state of charge (SOC) estimation with output outliers. First, a second-order resistance-capacitance (RC) equivalent circuit model is built to reflect the operating characteristics of the battery. Then, the APG method is applied to correct the output outliers. The FFRLS and extended Kalman filtering (EKF) are used to estimate the battery model parameters and SOC interactively. In order to verify the effectiveness of the proposed algorithm, this paper models the Samsung lithium battery and compares the effectiveness of different algorithms in estimating SOC. The experimental results show that the proposed APG-FFRLS-EKF algorithm has higher accuracy.

Keywords State of charge · Forgetting factor recursive least squares algorithm · Accelerated proximal gradient algorithm · Second-order RC model · Output with outliers

Introduction

Electric vehicles have emerged as a crucial direction in the development of environmentally friendly transportation, primarily due to their low emissions and energy-saving attributes [1, 2]. In the realm of electric vehicle power batteries, lithium batteries are extensively utilized owing to their notable advantages, including high specific energy and compact size [3, 4]. Within the battery management system, the state of charge (SOC) serves as a critical parameter, and precise estimation of SOC holds paramount significance in enhancing battery efficiency and safety performance [5, 6].

✉ Jing Chen
chenjing1981929@126.com

Xixi Ji
xixiji19981107@126.com

Zili Zhang
zhangzili1995@126.com

Yawen Mao
myw0530@163.com

1 School of Science, Jiangnan University, Wuxi 214122, People's Republic of China

2 School of Mechatronic Engineering and Automation, Shanghai University, Shanghai 200444, People's Republic of China

Nevertheless, in practical applications, the accurate estimation of SOC proves to be a formidable challenge due to the nonlinear characteristics inherent to batteries and the intricate nature of the external operating environment [7–9].

Several methods are available for estimating SOC, including the open circuit voltage method, particle filtering algorithm, neural network method, and Kalman filtering algorithm, among others [10–14]. The open-circuit voltage method exhibits high accuracy in estimating SOC during stationary states, but it is not suitable for real-time estimation [15]. On the other hand, the particle filtering algorithm offers accurate results but comes with high computational complexity, consuming significant computational resources [16]. The neural network method demonstrates high accuracy for a specific battery, but its adaptability to different battery types is limited due to variations in battery characteristics at the individual cell level [17]. Currently, the extended Kalman filter algorithm has emerged as a prominent research focus in battery management systems due to its simplicity in computation, high accuracy, and suitability for real-time SOC estimation [18–21].

In some control systems, such as distillation control and combustion process control, outliers may appear in the measurable data due to sensor failures or interrupted information transmission [22–25]. Outliers in the system output can

significantly decrease the accuracy of parameter identification or even lead to identification failure [26–30]. Therefore, in recent years, numerous scholars have developed a multitude of algorithms to address the issue of outliers. For example, Zhou et al. improved the autoregressive integral moving average (ARIMA) model and applied it to quality control of seafloor observations through sliding windows and cleaning of input modeling data [31]. Su et al. proposed OmniAnomaly, a stochastic recurrent neural network for multivariate time series anomaly detection, which reconstructs the input data through robust representation and uses the reconstruction probability to determine the outliers [32]. Peter et al. approximated the sum of squares of the residuals to create a least median of squares (LMS) algorithm [33].

In practical applications, the state of lithium batteries is prone to being influenced by the external working environment, leading to the presence of outliers in the process information matrix [16]. To address this issue, this paper introduces the APG algorithm, aiming to handle the state matrix that contains outliers [34, 35]. The fundamental concept of the APG algorithm involves iteratively approximating the low-rank structure of the original matrix [36]. The APG algorithm effectively recovers the outliers in the state matrix, transforming them into normal data [37, 38].

The contributions of this study are summarized below.

1. Introduce the APG algorithm to deal with state vectors containing outliers, which can improve the estimation accuracy of SOC.
2. Build the APG-FFRLS-EKF algorithmic framework for online interactive estimation of SOC, which is highly extensible.

The rest of this paper is structured as follows. "Model derivation" introduces the parameter identification model and the SOC estimation model. "SOC estimation based on APG-FFRLS-EKF algorithm" presents an APG-FFRLS-EKF algorithm for SOC estimation models with output outliers. In "Examples", an example for Samsung lithium batteries is provided. "Conclusions" summarizes this paper and gives future directions.

Model derivation

Parameter identification model

In this paper, we apply the second-order RC equivalent circuit model for the study. It can nicely simulate the charging and discharging behavior of lithium batteries [39, 40]. The basic structure of the model is shown in Fig. 1.

According to Kirchhoff's voltage-current law, the circuit physical quantities can be described as:

$$\begin{cases} i_L(t) = C_1 \dot{u}_1 + \frac{u_1(t)}{R_1}, \\ i_L(t) = C_2 \dot{u}_2 + \frac{u_2(t)}{R_2}, \\ u_L(t) = u_{ocv}(t) - i_L(t)R_0 - u_1(t) - u_2(t). \end{cases} \tag{1}$$

where u_L denotes the terminal voltage, u_{ocv} denotes the open circuit voltage, R_0 is a series resistance, R_1 is a polarization resistance, R_2 is a concentration polarization resistance, C_1 is a polarization capacitance, and C_2 is a concentration polarization capacitance.
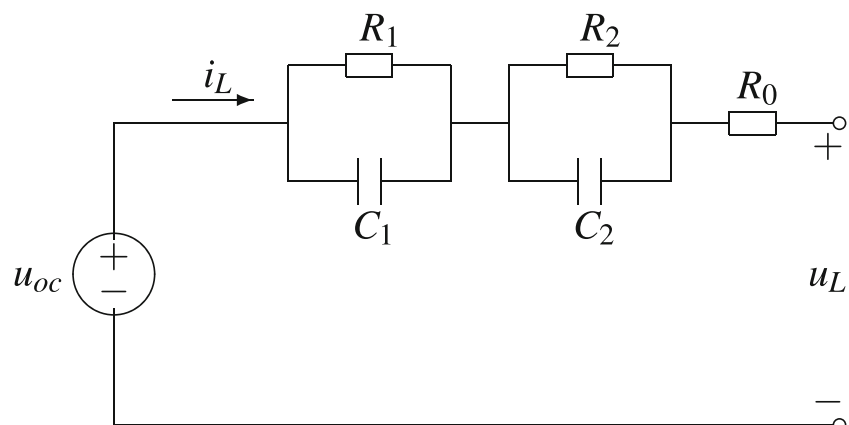
Applying the Laplace transform to Eq. 1, yields

$$\begin{cases} U_1(s) = \frac{I_L(s)R_1}{1+R_1C_1s}, \\ U_2(s) = \frac{I_L(s)R_2}{1+R_2C_2s}, \\ U_L(s) = U_{ocv}(s) - I_L(s)R_0 - U_1(s) - U_2(s). \end{cases} \tag{2}$$

Integrating the above equation, we get

$$U_{ocv}(s) = \left(\frac{R_1}{R_1C_1s+1} + \frac{R_2}{R_2C_2s+1} + R_0\right)I_L(s) + U_L(s). \tag{3}$$

Fig. 1 Schematic diagram of the second-order RC model

Transform the above equation into a differential equation and discretize it, and define

$$h(k) = u_{ocv}(k) - u_L(k), \tag{4}$$

$$\boldsymbol{\varphi}(k) = [h(k-1)\ h(k-2)\ i(k)\ i(k-1)\ i(k-2)]^{\mathrm{T}}, \tag{5}$$

$$U_L(s) = U_{ocv}(s) - I_L(s)R_0 - U_1(s) - U_2(s). \tag{6}$$

$\theta_1, \theta_2, \theta_3, \theta_4$ and θ_5 are expressed as follows.

$$\begin{cases} \theta_1 = \frac{8a_1 - 2}{1 + 2a_2 + 4a_1}, \\ \theta_2 = -\frac{1 - 2a_2 + 4a_1}{1 + 2a_2 + 4a_1}, \\ \theta_3 = -\frac{a_4 + 2a_3 + 4a_1 R_0}{1 + 2a_2 + 4a_1}, \\ \theta_4 = -\frac{2a_4 - 8a_1 R_0}{1 + 2a_2 + 4a_1}, \\ \theta_5 = -\frac{a_4 - 2a_3 + 4a_1 R_0}{1 + 2a_2 + 4a_1}, \end{cases} \tag{7}$$

and

$$\begin{cases} a_1 = R_1 C_1 R_2 C_2, \\ a_2 = R_1 C_1 + R_2 C_2, \\ a_3 = R_1 R_2 C_2 + R_1 C_1 R_2 + R_0 (R_1 C_1 + R_2 C_2), \\ a_4 = R_0 + R_1 + R_2. \end{cases} \tag{8}$$

Then, the battery model is simplified to the following linear form:

$$h(k) = \boldsymbol{\varphi}^{\mathrm{T}}(k)\boldsymbol{\theta}.$$

Since the open circuit voltage u_{ocv} is unknown, the parameters in the model cannot be estimated and need to be alternately estimated in conjunction with the SOC model.

SOC estimation model

The establishment of a lithium battery state space model is the fundamental for SOC estimation. The expression for the SOC of lithium batteries is given below:

$$SOC(t_1) = SOC(t_0) - \frac{1}{C_r} \int_{t_0}^{t_1} \eta i_L(t) dt, \tag{9}$$

where $SOC(t_1)$ denotes the battery SOC at the sampling moment t_1, C_r indicates the rated capacity of the battery, η is the Coulomb coefficient, and $i_L(t)$ denotes the current of the battery.

Combining Eqs. 1 and 7, we can get the state space model of lithium battery as follows.

$$\begin{cases} u_1(k+1) = e^{-\frac{\Delta t_{k+1}}{R_1 C_1}} u_1(k) + (1 - e^{-\frac{\Delta t_{k+1}}{R_1 C_1}}) R_1 i_L(k), \\ u_2(k+1) = e^{-\frac{\Delta t_{k+1}}{R_2 C_2}} u_2(k) + (1 - e^{-\frac{\Delta t_{k+1}}{R_2 C_2}}) R_2 i_L(k), \\ SOC(k+1) = SOC(k) - \frac{\eta t}{C_r} i_L(k), \\ u_L(k) = Q(SOC(k)) - u_1(k) - u_2(k) - R_0 i_L(k). \end{cases} \tag{10}$$

Considering the noise term, we can obtain the following discretized state space equation for SOC,

$$\begin{cases} \boldsymbol{x}(k+1) = \boldsymbol{A}(k)\boldsymbol{x}(k) + \boldsymbol{B}(k)i_L(k) + \boldsymbol{R}(k), \\ y(k) = \boldsymbol{C}(k)\boldsymbol{x}(k) + D(k)i_L(k) + V(k), \end{cases} \tag{11}$$

where

$$\boldsymbol{x}(k) = \begin{bmatrix} SOC(k) \\ u_1(k) \\ u_2(k) \end{bmatrix}, \quad \boldsymbol{A}(k) = \begin{bmatrix} 1 & 0 & 0 \\ 0 & e^{-\frac{\Delta t_{k+1}}{R_1 C_1}} & 0 \\ 0 & 0 & e^{-\frac{\Delta t_{k+1}}{R_2 C_2}} \end{bmatrix},$$

$$\boldsymbol{B}(k) = \begin{bmatrix} -\frac{\eta t}{C_r} \\ (1 - e^{-\frac{\Delta t_{k+1}}{R_1 C_1}}) R_1 \\ (1 - e^{-\frac{\Delta t_{k+1}}{R_2 C_2}}) R_2 \end{bmatrix}, \quad \boldsymbol{C}(k) = [-1\ -1\ \frac{\partial Q(SOC)}{\partial SOC}]^{\mathrm{T}},$$

$$D(k) = -R_0, \quad \boldsymbol{R}(k) = \begin{bmatrix} R_1(k) \\ R_2(k) \\ R_3(k) \end{bmatrix}.$$

$Q(\cdot)$ describes the relationship between SOC and u_{ocv}. At the $k - th$ moment, the process noise and the measurement noise are $\boldsymbol{R}(k)$ and $V(k)$, respectively.

The open-circuit voltage u_{ocv} and SOC of Li-ion batteries have a strong nonlinear relationship [39, 40]. This can be obtained by pulse charge and discharge tests, as shown in Fig. 2.

Remark 1 Batteries follow different curves between charging and discharging due to the hysteresis of the batteries. In this paper, the average of their curves is taken as the true $SOC - u_{ocv}$ relationship.

SOC estimation based on APG-FFRLS-EKF algorithm

In this section, we give an algorithmic framework for SOC estimation of lithium batteries containing outliers.

Terminal voltage recovery based on accelerated proximal gradient algorithm

In control systems such as chemical process control and network control, the problem of outliers in measured data sets often arises.

In the battery model parameter identification, the current and voltage information of the battery needs to be collected as the input and output of the model. Assume that the collected terminal voltages contain outliers due to operational errors or complex environments. In this paper, the accelerated proximal gradient algorithm is used to process the outliers.

Fig. 2 Battery SOC-OCV average curve under intermittent charge and discharge test
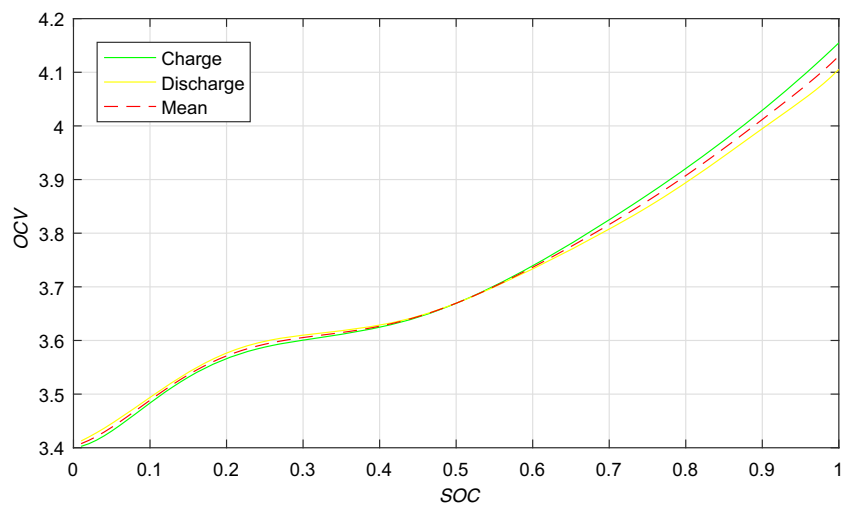
The APG algorithm is commonly used to solve Robust Principal Component Analysis (RPCA) problems [41]. It is widely used in computer vision fields such as face recognition and image recovery [42, 43].

The RPCA problem is mainly the following form.

$$\min_{A,E} \ \|A\|_* + \lambda \|E\|_1 \quad s.t. \ D = A + E, \tag{12}$$

where D is the measurable matrix, A is the recovered low-rank matrix, and E is the sparse matrix.

The APG algorithm is used to solve the above problem. It is an iterative algorithm commonly used in optimization problems to recover low-rank matrices. The idea is to gradually approximate the optimal solution by alternately updating the matrix and the estimated gradient, combining the most closest estimate and the most closest gradient in each step.

By the definition in "Model derivation", let $u_L(1), ..., u_L(M)$ be the collected terminal voltages. In this case, $\bar{u}_L(l_1), ..., \bar{u}_L(l_m)$ are the outliers.

First, the terminal voltage vector $\left[u_L(1), ..., u_L(M)\right]^{\mathrm{T}}$ is converted to a matrix $\bar{\Phi}$, where

$$\bar{\Phi} = \begin{bmatrix} u_L(1) & u_L(n+1) & ... & u_L(M-n+1) \\ ... & ... & ... & ... \\ u_L(n) & u_L(2n) & ... & u_L(M) \end{bmatrix}.$$

Then, we can recover the terminal voltage matrix with outliers $\bar{\Phi}$ to Φ by the APG algorithm.

The APG algorithm is intended to solve the following optimization problem.

$$\min_{\Phi,E} \ \|\Phi\|_* + \lambda \|E\|_1 \quad s.t. \ \bar{\Phi} = \Phi + E, \tag{13}$$

where E is a sparse matrix and λ is a penalty factor.

Define $W = (\Phi, E)$, $f(W) = \dfrac{\left\|\bar{\Phi} - \Phi - E\right\|_F^2}{2}$ and $g(W) = \mu \|\Phi\|_* + \lambda\mu \|E\|_1$. From Eq. 10, we construct the following Lagrangian function.

$$G(W) = g(W) + f(W)$$
$$= \mu \|\Phi\|_* + \lambda\mu \|E\|_1 + \frac{\left\|\bar{\Phi} - \Phi - E\right\|_F^2}{2},$$

where μ is a relaxation factor.

Lemma 1 [44] *Approximate $G(W)$ at the point W using the quadratic separable sequence $Q(W, \widetilde{W})$. The expression for $Q(W, \widetilde{W})$ is:*

$$Q(W, \widetilde{W}) = g(W) + f(\widetilde{W}) +$$
$$< \nabla f(\widetilde{W}), W - \widetilde{W} > + \frac{L_f}{2} \left\| W - \widetilde{W} \right\|^2,$$

where $< \nabla f(\widetilde{W}), W - \widetilde{W} >= tr(\nabla f^{\mathrm{T}}(\widetilde{W})(W - \widetilde{W}))$ and L_f is the Lipschitz constant of $f(W)$.

Minimizing $G(W)$ is equivalent to minimizing $Q(W, \widetilde{W})$ in Lemma 1. *Define $D \doteq \widetilde{W} - \frac{1}{L_f} \nabla f(\widetilde{W})$, then we have*

$$\underset{W}{\mathrm{argmin}} \ Q(W, \widetilde{W}) = \underset{W}{\mathrm{argmin}} \left\{ g(W) + \frac{L_f}{2} \|W - D\|^2 \right\}. \tag{14}$$

Remark 2 If $\widetilde{W}_k = W_k$, the APG algorithm will degrade to a gradient descent algorithm.

The steps of the APG algorithm contain alternate updates to Φ and E. According to Eq. 11, E can be solved as follows.

$$\underset{E}{\mathrm{argmin}} \left\{ \mu\lambda \|E\|_1 + \frac{L_f}{2} \left\| \bar{\Phi} - \Phi - E \right\|_F^2 \right\}.$$

Define

$$S_\tau[i] \doteq \begin{cases} i - \tau, & if\ i > \tau, \\ i + \tau, & if\ i < -\tau, \\ 0, & otherwise, \end{cases}$$

where $i \in \mathbb{R}$ and $\tau > 0$. According to the definition above, at the $(k + 1)$th iteration, let $D_k = (D_k^A, D_k^E)$, then E_{k+1} is updated according to the following equation.

$$E_{k+1} = S_{\frac{\lambda\mu}{L_f}} \left[D_k^E \right]. \tag{15}$$

Similarly, Φ can be computed by

$$\underset{\Phi}{\mathrm{argmin}} \left\{ \mu \|\Phi\|_* + \frac{L_f}{2} \left\| \bar{\Phi} - \Phi - E \right\|_F^2 \right\},$$

let $U S V^T$ be the singular value decomposition of D_k^A, then

$$\Phi_{k+1} = U S_{\frac{\lambda\mu}{L_f}} \left[D_k^A \right] V^T. \tag{16}$$

Remark 3 In the APG algorithm, by setting $t_{k+1} = \frac{1 + \sqrt{4t_k^2 + 1}}{2}$, the convergence rate can reach quadratic convergence [45].
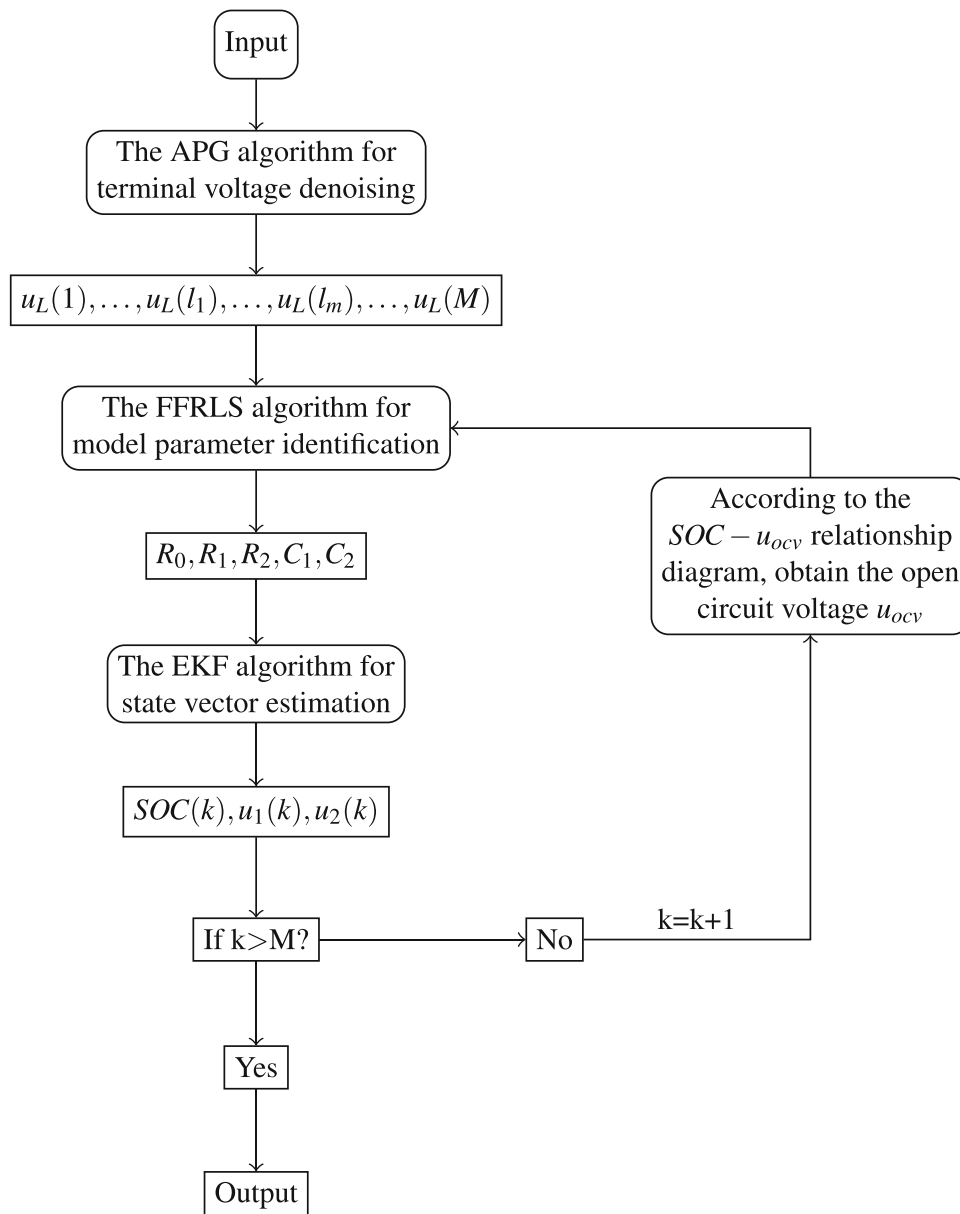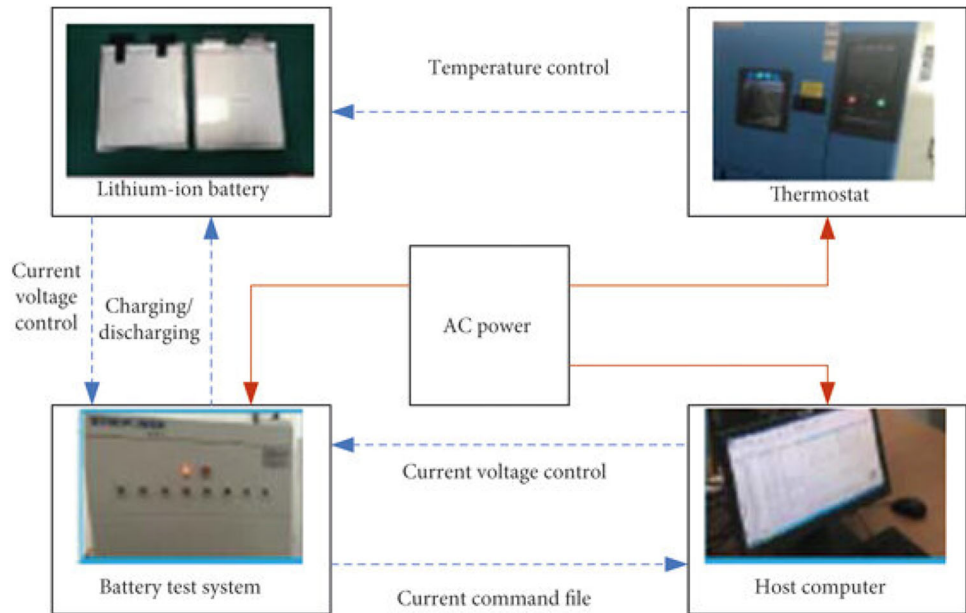

Fig. 3 The framework of the APG-FFRLS-EKF algorithm

Fig. 4 The battery test platform

We summarize the APG algorithm as Algorithm 1.

Algorithm 1 APG algorithm.

1: **Input:** Expanded matrix $\bar{\Phi}$.
2: Initialization: $t_0, t_{-1} \leftarrow 1$; $\Phi_0, \Phi_{-1} \leftarrow \mathbf{0}$; $E_0, E_{-1} \leftarrow \mathbf{0}$.
3: **repeat**
4:     $k \leftarrow k + 1$
5:     Update E_{k+1} based on Eq. 13.
6:     Update Φ_{k+1} based on Eq. 14.
7:     Update t_{k+1} by $t_{k+1} \leftarrow \frac{1+\sqrt{4t_k^2+1}}{2}$.
8: **until** $\left\| \bar{\Phi} - \Phi_k - E_k \right\|_F / \left\| \bar{\Phi} \right\|_F < \varepsilon$.
Output: $\Phi \leftarrow \Phi_k$, $E \leftarrow E_k$.

The APG-FFRLS-EKF algorithm for SOC

When there are outliers in the terminal voltages of the output data, traditional identification algorithms have low efficiency and accuracy. The APG-FFRLS-EKF algorithm solves this problem by recovering the outliers in the terminal voltages. Compared with the traditional SOC estimation method, it not only improves the estimation accuracy of the identification model, but also decreases the error of SOC estimation.

In this section, the APG-FFRLS-EKF algorithm for SOC estimation of output voltages containing outliers is presented in detail.

First, the APG algorithm is used to recover the terminal voltage outliers. Then, the model parameters R_0, R_1, R_2, C_1, C_2 are estimated using the FFRLS algorithm. In this case, the open circuit voltage u_{ocv} in the output data can be obtained from the relationship between SOC and u_{ocv}. The model

parameters are identified so that they can be used to alternatively estimate the SOC.

In summary, the steps of the APG-FFRLS-EKF algorithm are as in Algorithm 2.

1. Collect current and terminal voltage data $\{i_L(1), u_L(1)\}$ ... $\{i_L(M), u_L(M)\}$ from lithium batteries, where $\bar{u}_L(l_1)$, ..., $\bar{u}_L(l_m)$ is the sequence of outliers.
2. Expand the terminal voltage vector $[u_L(1), ...\bar{u}_L(l_1), ..., \bar{u}_L(l_m), ...u_L(M)]^T$ as a matrix $\bar{\Phi}$.
3. Use the APG algorithm to recover the matrix $\bar{\Phi}$ into a clean matrix Φ. Φ is then vectorized to $[u_L(1), ...\hat{u}_L(l_1), ..., \hat{u}_L(l_m), ...u_L(M)]^T$, where $[\hat{u}_L(l_1), ..., \hat{u}_L(l_m)]^T$ is the recovered terminal voltage vector.
4. Initialize $\theta(0)$, $P(0)$, $SOC(0)$ and $x(0)$.
5. Get $u_{ocv}(0)$ from the nonlinear relationship between u_{ocv} and SOC. Obtain $h(k)$ based on the terminal voltages obtained from step 3 and Eq. 4.
6. Obtain the observation vector $\varphi(k)$ according to Eq. 5.

Table 1 The parameters of NCR18650PF

Capacity	2900 mAh
Normal voltage	3.63 V
Min/max voltage	2.75 V/4.2 V
Standard charge/rapid charge	1.3 A/2.6 A
Max charge current	2.6 A
Max discharge current	5.2 A
Operating discharge temperature	$-20°C/60°C$
Dimensions	18.00*65.00 mm

Fig. 5 Intermittent current
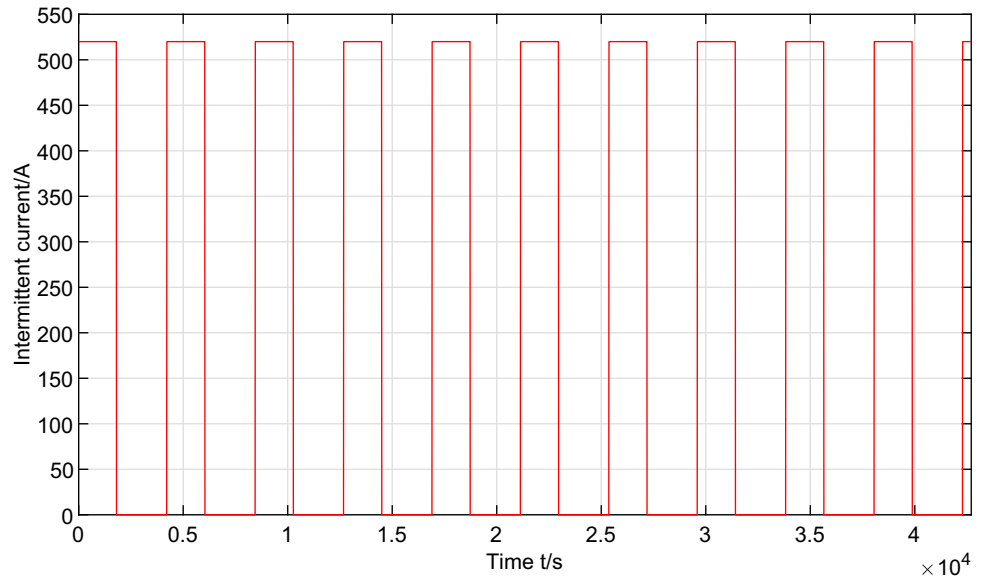
7. Compute the gain matrix:

$$L(k) = \frac{P(k-1)\varphi(k)}{\lambda + \varphi^T(k)P(k-1)\varphi(k)}, \quad (17)$$

update parameter estimation:

$$\hat{\theta}(k) = \hat{\theta}(k-1) + L(k)[h(k) - \varphi^T(k)\hat{\theta}(k-1)], \quad (18)$$

update the covariance matrix:

$$P(k) = [I - L(k)\varphi^T(k)]P(k-1). \quad (19)$$

Obtain the battery model parameters R_0, R_1, R_2, C_1, C_2 according to Eqs. 7 and 8.

8. Substitute the battery model parameters obtained from step 7 into Eq. 11.
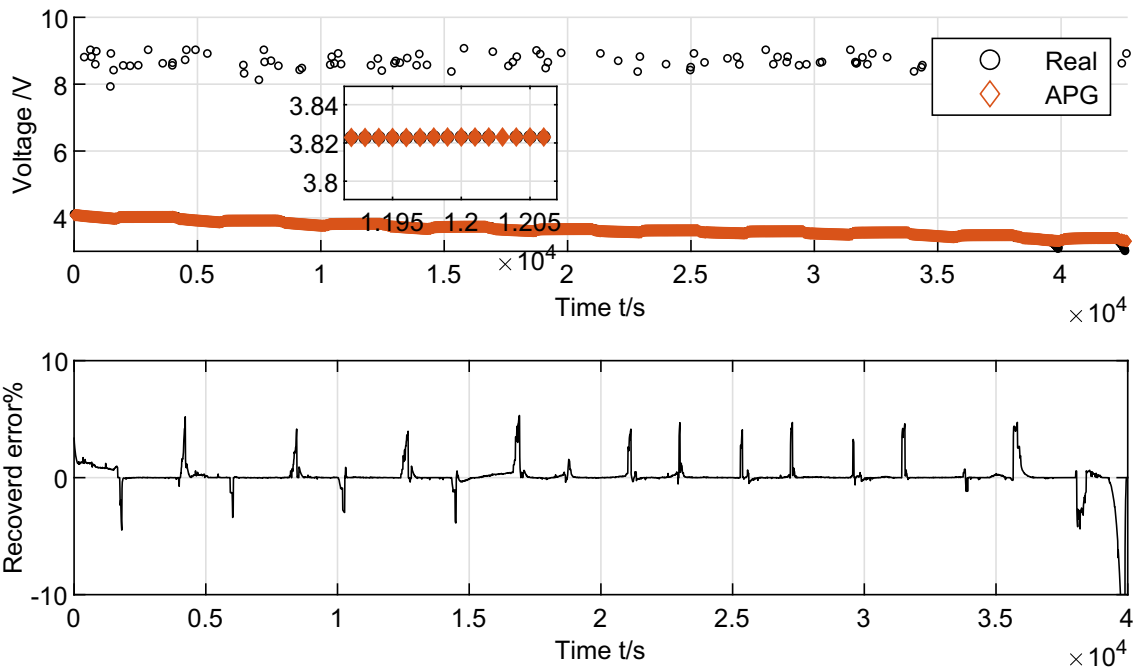
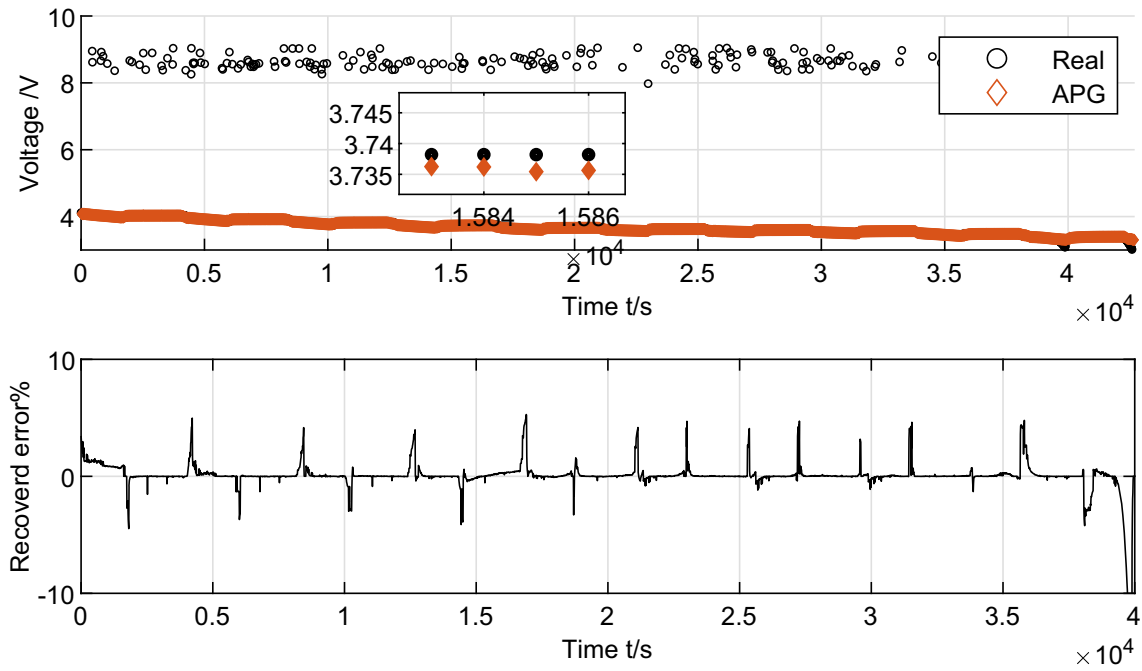**Fig. 6** Output estimates and errors with number of outliers 100

Fig. 7 Output estimates and errors with number of outliers 200

9. Make predictions about the state vector and the covariance matrix:

$$\hat{\boldsymbol{x}}^-(k) = \boldsymbol{A}(k-1)\hat{\boldsymbol{x}}(k-1) + \boldsymbol{B}(k-1)i_L(k-1), \quad (20)$$
$$\widetilde{\boldsymbol{P}}^-(k) = \boldsymbol{A}(k-1)\widetilde{\boldsymbol{P}}^-(k-1)\boldsymbol{A}^{\mathrm{T}}(k-1) + \boldsymbol{V}(k-1). \quad (21)$$

10. Gain Kalman Gain:

$$\boldsymbol{K}(k) = \widetilde{\boldsymbol{P}}^-(k)\boldsymbol{C}^{\mathrm{T}}(k)[\boldsymbol{C}(k)\widetilde{\boldsymbol{P}}^-(k)\boldsymbol{C}^{\mathrm{T}}(k) + \boldsymbol{V}(k)]^{\mathrm{T}}. \quad (22)$$
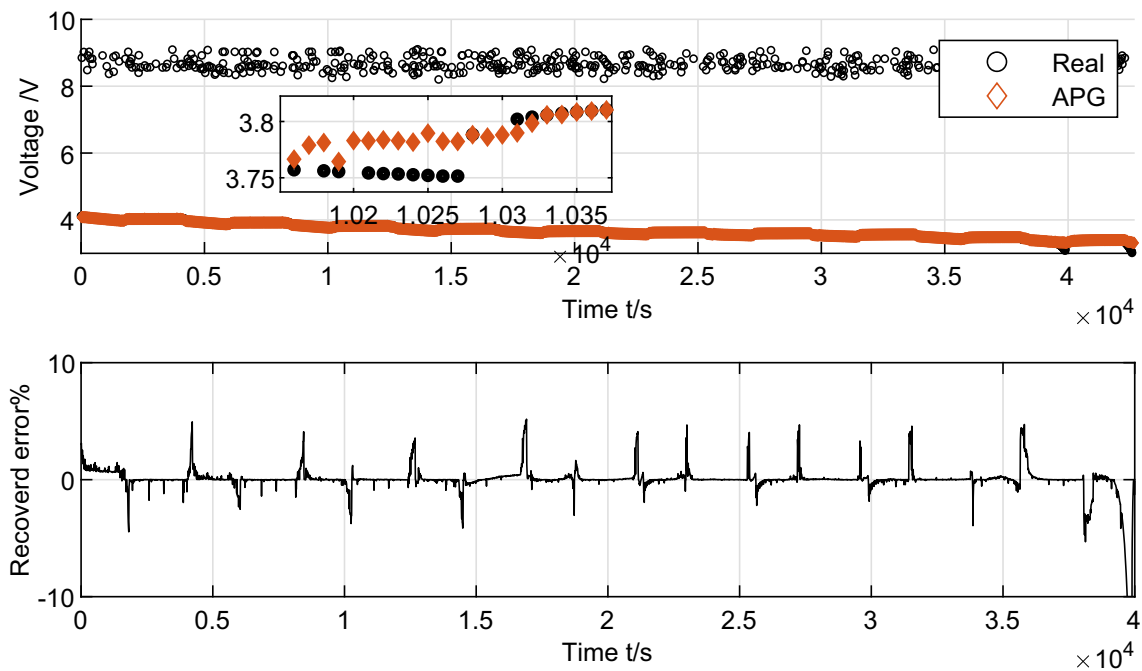
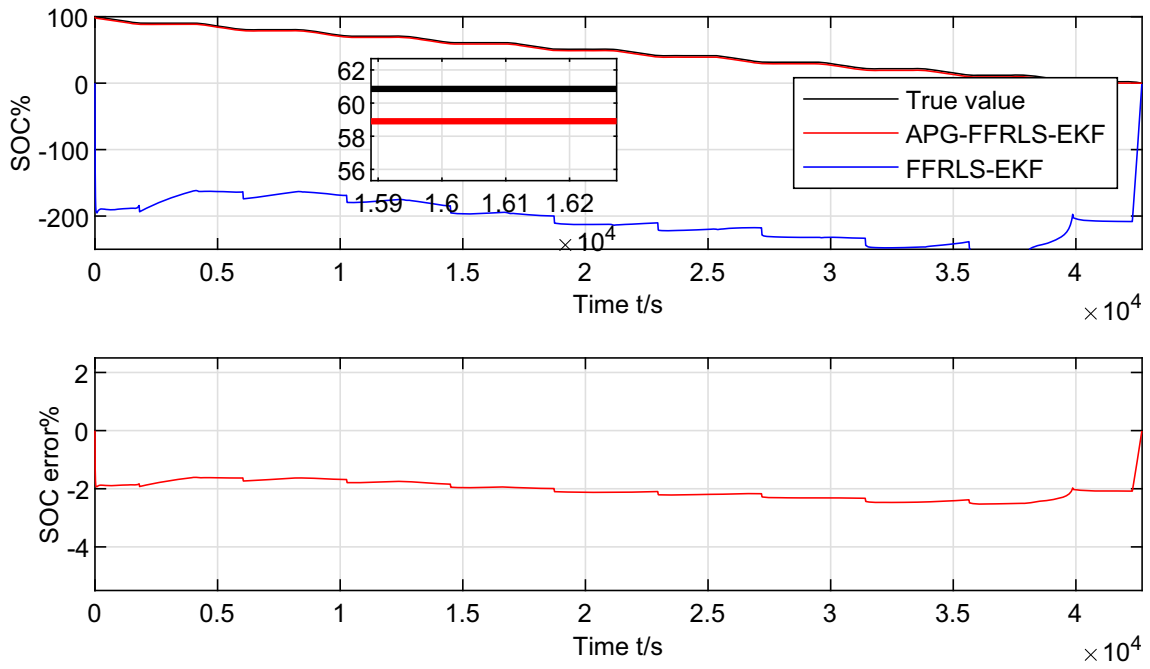**Fig. 8** Output estimates and errors with number of outliers 500

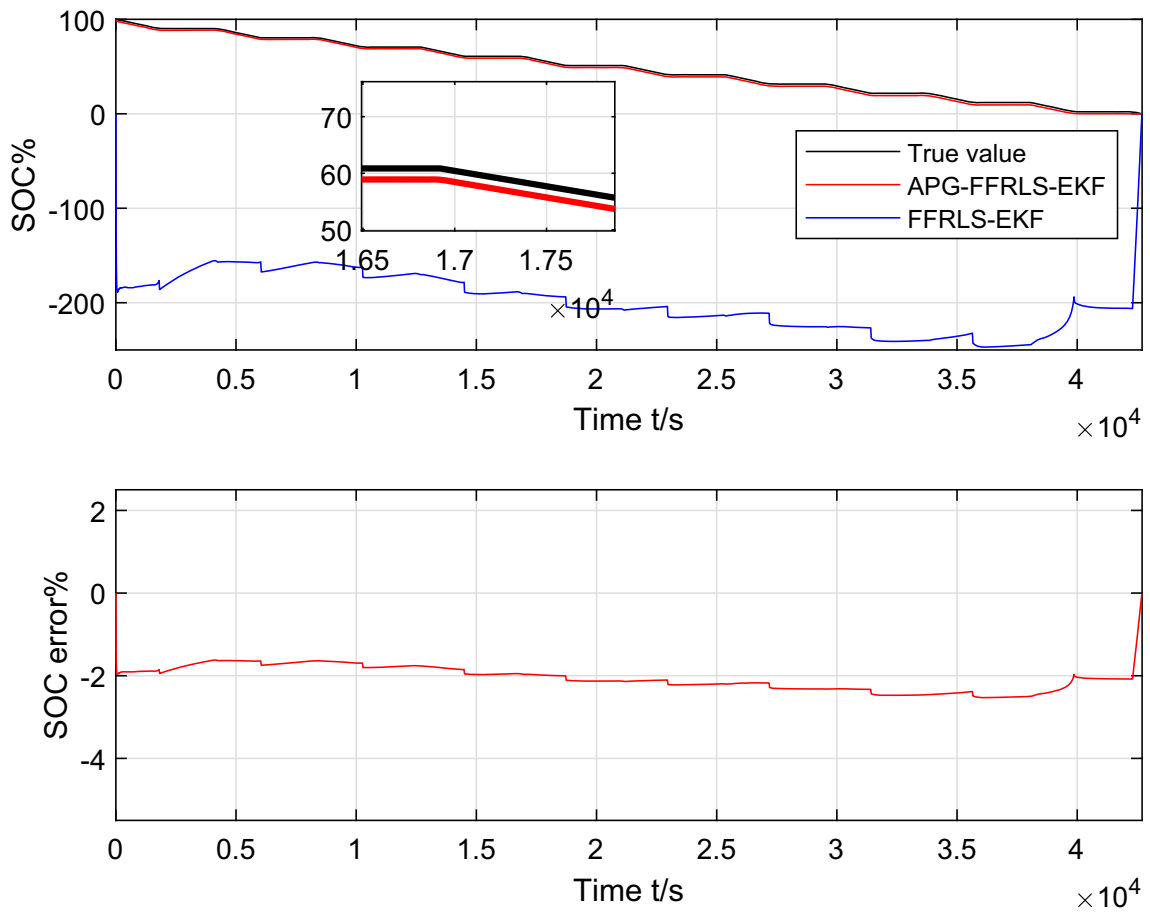**Fig. 9** SOC estimates and errors with number of outliers 100

Fig. 10 SOC estimates and errors with number of outliers 200

11. Update the state vector:

$$\hat{x}(k) = \hat{x}^-(k) + K(k)[y(k) - C(k)\hat{x}^-(k) - D(k)i_L(k)], \tag{23}$$

where $\hat{x}(k) = [SOC(k)\ u_1(k)\ u_2(k)]^T$.

12. Update the covariance matrix:

$$\widetilde{P}(k) = [I - K(k)C(k)]\widetilde{P}^-(k). \tag{24}$$

13. If $k \geqslant M$, then take up the state vector $\hat{x}(k)$; otherwise, let $k = k + 1$ and go back to step 5.

The framework of the APG-FFRLS-EKF algorithm is shown in Fig. 3.

Examples

The battery tester platform

In order to verify the accuracy of the APG-FFRLS-EKF algorithm in SOC estimation of Li-ion batteries, discharge trial experiments are conducted. As shown in Fig. 4, lithium-ion batteries are tested using the battery experimental platform. The experiments are conducted at room temperature of 25°C during the whole process. The battery experiment platform

includes a battery tester, a battery holder, Samsung lithium-ion batteries and a host computer. The main parameters of the Samsung lithium-ion battery are shown in Table 1.

Experiments and analysis

Intermittent discharge experiments are conducted on lithium batteries to obtain current and voltage data by sampling. Battery discharge tests were performed at the current profiles shown in Fig. 5.

Generate 100, 200, and 500 random numbers, respectively, to simulate the case of different numbers of outliers in the battery terminal voltage data. The APG-FFRLS-EKF algorithm and FFRLS-EKF algorithm are applied to estimate the output voltage with outliers and SOC.

Under the influence of different numbers of outliers, the output estimates and errors are shown in Figs. 6, 7, and 8. The SOC estimates and errors are shown in Figs. 9, 10, and 11. From Figs. 6, 7, and 8, it can be seen that the terminal voltage data after recovery by the APG algorithm is close to normal. When the percentage of outliers is close to 3%, the data after APG recovery is almost normal. When the percentage of outliers is more than 10%, the data after APG recovery is still close to normal.

From Table 2, it can be seen that the proposed APG-FFRLS-EKF algorithm can obtain high SOC estimation accuracy, with MAE less than 2.0787, and RMSE less than 2.0986.
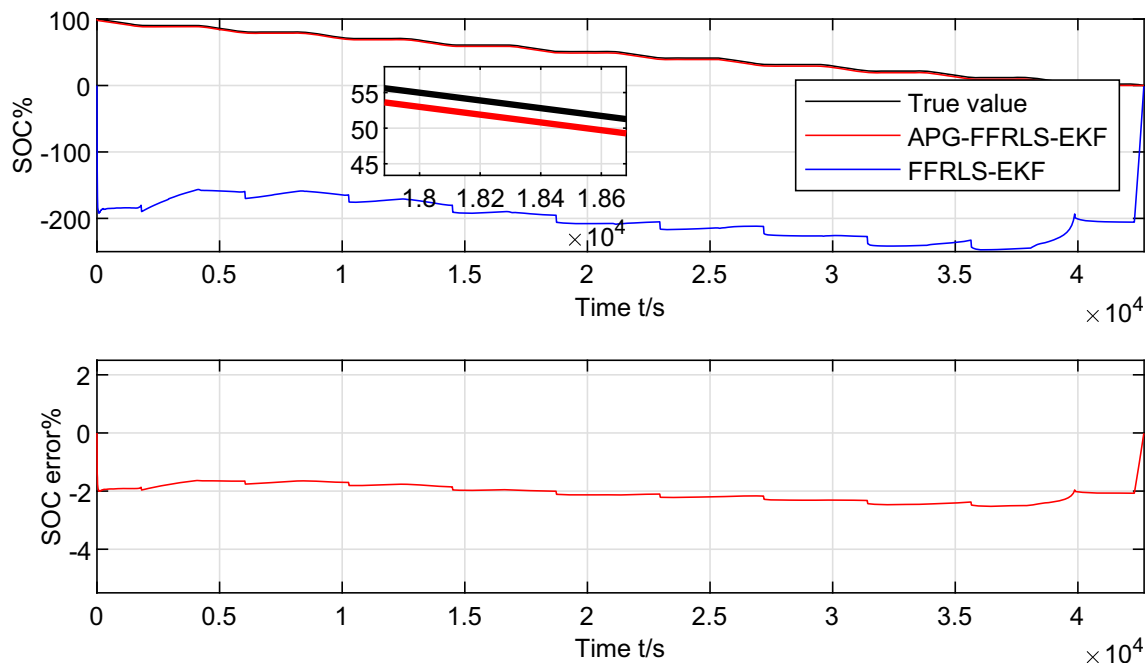

Fig. 11 SOC estimates and errors with number of outliers 500

Table 2 Estimation errors of SOC

Number of outliers	100	200	500
MAE	2.0605	2.0649	2.0787
RMSE	2.0825	2.0863	2.0986

Conclusions

An APG-FFRLS-EKF algorithm is proposed for the problem of SOC estimation of lithium batteries with output outliers. The APG-FFRLS-EKF algorithm polishes the outlier outputs in advance, which can lead to higher SOC estimation accuracy. Compared with the traditional SOC estimation method, this method has more accurate estimation accuracy and is more robust. It should be noted that the theoretical proof of the convergence analysis of the APG-FFRLS-EKF algorithm is challenging and deserves further study.

Data Availability No datasets were generated or analyzed during the current study.

Declarations

Ethics approval This study does not involve human and/or animal studies.

Conflict of interest The authors declare no competing interests.

References

1. Jiao M, Yang Y, Wang DQ, Gong P (2021) The conjugate gradient optimized regularized extreme learning machine for estimating state of charge. Ionics 27(11):4839–4848
2. Lu JB, He YF, Liang HS, Li MG, Shi ZN, Zhou K, Li ZD, Gong XX, Yuan GQ (2023) State of charge estimation for energy storage lithium-ion batteries based on gated recurrent unit neural network and adaptive Savitzky-Golay filter. Ionics 29(10):1–14
3. Belaid S, Rekioua D, Oubelaid A, Ziane D, Rekioua T (2022) A power management control and optimization of a wind turbine with battery storage system. J Energy Storage 45:103613
4. Preger Y, Loraine TC, Rauhala T, Jeevarajan J (2022) Perspective on the safety of aged Lithium-ion batteries. J Electrochem Soc 169(3):030507
5. Hossain LMS, Hannan MA, Hussain A, Hoque MM, Pin KJ, Saad MHM, Ayob A (2018) A review of state of health and remaining useful life estimation methods for lithium-ion battery in electric vehicles: Challenges and recommendations. J Clean Prod 205:115–133
6. Kim T, Ochoa J, Faika T, Mantooth HA, Di J, Li QH, Lee Y (2020) An overview of cyber-physical security of Battery management systems and adoption of Blockchain technology. IEEE J Emerg Sel Top Power Electron 10(1):1270–1281
7. Hannan MA, Hoque MM, Hussain A, Yusof Y, Ker PJ (2018) State-of-the-art and energy management system of Lithium-ion batteries in electric vehicle applications: issues and recommendations. IEEE Access 6:19362–193781
8. Gan M, Chen XX, Ding F, Chen GY, Chen CLP (2019) Adaptive RBF-AR models based on multi-innovation least squares method. IEEE Signal Process Lett 26(8):1182–1186
9. Ng KS, Moo CS, Chen YP, Hsieh YC (2009) Enhanced coulomb counting method for estimating state-of-charge and state-of-health of lithium-ion batteries. Appl Energy 86(9):1506–1511
10. Cho BH, Kim J, Shin J, Chun C (2011) Stable configuration of a li-ion series battery pack based on a screening process for improved voltage/SOC balancing. IEEE Trans Power Electron 27(1):411–424
11. Seongjun L, Jonghoon K, Jaemoon L, Cho BH (2008) State-of-charge and capacity estimation of lithium-ion battery using a new open-circuit voltage versus state-of-charge. J Power Sources 185(2):1367–1373
12. Xia BZ, Sun Z, Zhang RF, Lao ZZ (2017) A cubature particle filter algorithm to estimate the state of the charge of Lithium-ion batteries based on a second-order equivalent circuit model. Energies 10(4):1–15
13. Shen XF, Wang SL, Yu CM, Qi CS, Li ZH, Fernandez C (2023) A hybrid algorithm based on beluga whale optimization-forgetting factor recursive least square and improved particle filter for the state of charge estimation of lithium-ion batteries. Ionics 29(10):4351–4363
14. Andre D, Nuhic A, Guth TS (2013) Comparative study of a structured neural network and an extended Kalman filter for state of health determination of lithium-ion batteries in hybrid electricvehicles. Eng Appl Artif Intell 26(3):951–961
15. Zhu T, Wang SL, Fan YC, Zhou H, Zhou YF, Fernandez C (2023) Improved forgetting factor recursive least square and adaptive square root unscented Kalman filtering methods for online model parameter identification and joint estimation of state of charge and state of energy of lithium-ion batteries. Ionics 29(9):5295–5314
16. Zhang ZL, Chen J, Mao YW, Liao CC (2023) Improved square root cubature Kalman filter for state of charge estimation with state vector outliers. Ionics 29(10):1369–1379
17. Jiao M, Wang DQ, Qiu J (2021) More intelligent and robust estimation of battery state-of-charge with an improved regularized extreme learning machine. Eng Appl Artif Intell 104:104407
18. Kalman RE (1960) A new approach to linear filtering and prediction problems. J Fluids Eng 82(1):35–45
19. Middleton R, Freeston M, McNeill L (2004) An application of the extended Kalman filter to robot soccer localisation and world modelling. IFAC Proc Volumes 37(14):729–734
20. Ribeiro MI, Ribeiro I (2004) Kalman and extended Kalman filters: concept, derivation and properties. Institute Syst Robotics 43(46):3736–3741
21. Einicke GA, White LB (1999) Robust extended Kalman filtering. IEEE Trans Signal Process 47(9):2596–2599
22. Wang DQ, Li LW, Ji Y, Yan YR (2018) Model recovery for Hammerstein systems using the auxiliary model based orthogonal matching pursuit method. Appl Math Model 54:537–550
23. Chen J, Zhu QM, Liu YJ (2020) Modified Kalman filtering based multi-step-length gradient iterative algorithm for ARX models with random missing outputs. Automatica 118:109034
24. Chen J, Huang B, Gan M, Chen CLP (2021) A novel reduced-order algorithm for rational model based on Arnoldi process and Krylov subspace. Automatica 129:109663

25. Guo J, Jia RZ, Su RN, Zhao YL (2023) Identification of FIR systems with binary-valued observations against data tampering attacks. IEEE Trans Syst Man Cybern Syst. https://doi.org/10.1109/TSMC.2023.3276352

26. Chen J, Ding F, Zhu QM, Liu YJ (2019) Interval error correction auxiliary model based gradient iterative algorithms for multirate ARX models. IEEE Trans Autom Control 65(10):4385–4392

27. Liu XP, Yang XQ (2023) Variational identification of linearly parameterized nonlinear state-space systems. IEEE Trans Control Syst Technol 31(4):1844–1854

28. Ding F, Liu GJ, Liu XP (2011) Parameter estimation with scarce measurements. Automatica 47(8):1646–1655

29. Liu XP, Yang XQ (2023) Exploiting spike-and-slab prior for variational estimation of nonlinear systems. IEEE Trans Ind Inform 19(11):11275–11285

30. Liu XP, Yang XQ (2022) Identification of nonlinear state-space systems with skewed measurement noises. IEEE Trans Circuits Syst I: Regul Pap 69(11):4654–4662

31. Zhou YS, Qin RF, Xu HP, Sadiq S (2018) A data quality control method for seafloor observatories: the application of observed time series data in the East China Sea. Sensors 18(8)

32. Su Y, Zhao YJ, Niu CH, Liu R, Sun W, Pei D (2019) Robust anomaly detection for multivariate time series through stochastic recurrent neural network. Proceedings of the 25th ACM SIGKDD international conference on knowledge discovery and data mining, pp 2828-2837

33. Rousseeuw PJ (2012) Least median of squares regression. J Am Stat Assoc 79(388):871–880

34. Ellis SP (2000) Singularity and outliers in linear regression with application to least squares, least absolute deviation, and least median of squares linear regression. Metron 58(1):121–129

35. Basri R, Jacobs DW (2003) Lambertian reflectance and linear subspaces. IEEE Trans Pattern Anal Mach Intell 25(2):218–233

36. Candès EJ, Recht B (2008) Exact low-rank matrix completion via convex optimization. 2008 46th Annual Allerton Conference on Communication, Control, and Computing IEEE

37. Cai JF, Candès EJ, Shen ZW (2008) A singular value thresholding algorithm for matrix completion. SIAM J Optim 20(4):1956–1982

38. Elad M (2010) Sparse and redundant representations. Springer

39. Nuhic A, Terzimehic T, Guth TS, Buchholz M, Dietmayer K (2013) Health diagnosis and remaining useful life prognostics of lithium-ion batteries using data-driven methods. J Power Sources 239:680–688

40. Kim J, Lee SJ, Cho BH (2011) Complementary cooperation algorithm based on DEKF based pattern recognition for SOC/capacity estimation and SOH prediction. IEEE Trans Power Electron 27(1):436–451

41. Lin Z, Chen M, Ma Y (2013) The augmented lagrange multiplier method for exact recovery of corrupted low-rank matrices. Mathematics

42. Candès EJ, Li X, Ma Y et al (2009) Robust principal component analysis? J ACM 58(3):1–39

43. Lu X, Gong T, Yan P et al (2012) Robust alternative minimization for matrix completion. IEEE Trans Syst Man Cybern 42(3):939–949

44. Chen M (2009) Fast convex optimization algorithms for exact recovery of a corrupted low-rank matrix. Journal of the Marine Biological Association of the UK

45. Amir B, Marc T (2009) A fast iterative shrinkage-thresholding algorithm for linear inverse problems. SIAM J Imaging Sci 2(1):183–202